Caravan, R. L., Khan, A., Rotavera, B., Papajak, E., Antonov, I. O., Chen, M-W., Au, K., Chao, W., Osborn, D. L., Lin, J. J-M., Percival, C. J., Shallcross, D., & Taatjes, C. A. (2017). Products of Criegee intermediate reactions with NO2: experimental measurements and tropospheric implications. *Faraday Discussions*, *200*, 313-330. https://doi.org/10.1039/C7FD00007C

**Products of Criegee Intermediate Reactions with $NO_2$: Experimental Measurements and Tropospheric Implications**

Rebecca L. Caravan,[a] M. Anwar H. Khan,[b] Brandon Rotavera,[a] Ewa Papajak,[a] Ivan O. Antonov,[a] Ming-Wei Chen,[a] Kendrew Au,[a] Wen Chao,[c,d] David L. Osborn,[a] Jim Jr-Min Lin,[c,d] Carl J. Percival,[e] Dudley E. Shallcross,[b] Craig A. Taatjes[a]

*[a]Combustion Research Facility, Mailstop 9055, Sandia National Laboratories, Livermore, California, 94551 USA; [b]School of Chemistry, University of Bristol, Bristol BS8 1TS, UK; [c]Institute of Atomic and Molecular Sciences, Academia Sinica, Taipei 10617, Taiwan; [d]Department of Chemistry, National Taiwan University, Taipei 10617, Taiwan; [e]School of Earth, Atmospheric and Environmental Sciences, University of Manchester, Williamson Building, Oxford Road, Manchester M13 9PL, UK.*

**Abstract**

The reactions of Criegee intermediates with $NO_2$ have been proposed as a potentially significant source of the important nighttime oxidant $NO_3$, particularly in urban environments where concentrations of ozone, alkenes and $NO_x$ are high. However, previous efforts to characterize the yield of $NO_3$ from these reactions have been inconclusive, with many studies failing to detect $NO_3$. In the present work, the reactions of formaldehyde oxide ($CH_2OO$) and acetaldehyde oxide ($CH_3CHOO$) with $NO_2$ are revisited to further explore the product formation over a pressure range of 4-40 Torr. $NO_3$ is not observed; however, temporally resolved and $[NO_2]$-dependent signal is observed at the mass of the Criegee-$NO_2$ adduct for both formaldehyde- and acetaldehyde- oxide systems, and possible structures of the acetaldehyde oxide – $NO_2$ adduct are explored through *ab initio* calculations. The atmospheric implications of the title reaction are investigated through global modelling.

**Introduction**

The fates of many anthropogenic trace gas pollutants impacting health and climate are controlled by chemical oxidation in the troposphere.[1] For example, $NO_x$ lifetimes, which governs their impact on a global and regional scale, are fundamentally controlled by production of nitric acid ($HNO_3$) and organic nitrates, the latter of which extend both the lifetime and

spatial extent of $NO_x$. The nitrate radical ($NO_3$) is a crucial oxidant in the nighttime troposphere and is formed mainly from the reaction of $NO_2$ with ozone. Criegee intermediates, which originate principally from ozonolysis of alkenes, could have a significant impact on the $NO_x/NO_y$ budget on urban environments which are typically rich in $NO_x$, $O_3$ and alkenes. Direct measurements of the reaction of Criegee intermediates with $NO_2$ (R1) have shown that the rate coefficients are substantially faster than many previous estimates, with values on the order of $2 \times 10^{-12}$ molecule$^{-1}$ cm$^3$ s$^{-1}$ for formaldehyde-, acetaldehyde-, and acetone-oxides.[2-4] Using these rate coefficients, Vereecken *et al.* [5] estimated the potential loss of *syn*-acetaldehyde oxide via reaction with $NO_2$ to be as high as 22 % of the total *syn*-acetaldehyde oxide removal in mega cities where $NO_x$ emissions are high.

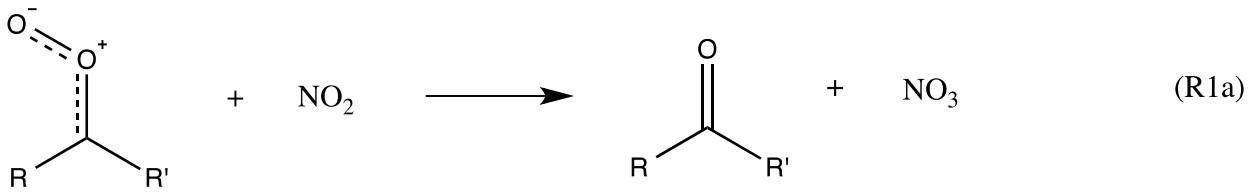


(R1a)


(R1b)

The $NO_3$ formation from reaction of Criegee intermediates could be to up to 40% of that produced from the $O_3 + NO_2$ reaction in the nocturnal boundary layer, if it is assumed that the reactions proceed exclusively via channel R1a.[3] It is difficult, however, to assess the atmospheric importance of these reactions as the branching fraction of $NO_3$ is poorly constrained, and laboratory studies of Criegee + $NO_2$ reactions have generated conflicting results.

Following investigations of ozonolysis products of tetramethylethylene (TME, 2,3-dimethyl-2-butene) in the presence of $NO_2$, Presto and Donahue[6] postulated that the yield of $NO_3$ from reaction with acetone oxide must be high based on their observation of enhanced acetone yields with increasing pressure and TME consumption.

The advent of methods for *in situ* production of Criegee intermediates via photolysis of diiodoalkane compounds in the presence of oxygen has facilitated direct studies of Criegee

intermediate kinetics, including of the title reaction.[7] Multiplexed photoionization mass spectrometry (MPIMS) measurements by Taatjes *et al.*[3] and Chhantyal-Pun *et al.*[2] on the acetaldehyde- and acetone-oxide systems, respectively, were unable to detect $NO_3$ as a reaction product, and furthermore, noted a decrease in the corresponding aldehyde/ketone signal with increasing $NO_2$ concentration. This is consistent with observations made by Stone *et al.*[4] in the study of the formaldehyde oxide reaction via laser-flash photolysis-laser-induced fluorescence spectroscopy, where reduction in formaldehyde signal with increasing $NO_2$ was attributed to the formation of $CH_2IO_2NO_2$, which is thought to inhibit formaldehyde formation.

Only the work of Ouyang *et al.*[8] has provided evidence for $NO_3$ production in the Criegee + $NO_2$ reactions following photolytic production of formaldehyde oxide. Under their reaction conditions, $NO_3$ was anticipated to be titrated to $N_2O_5$ via reaction with $NO_2$ and so simultaneous detection of $NO_3$ and ($NO_3$ + $N_2O_5$) was performed using steady-state Broadband Cavity Enhanced Absorption Spectrometry coupled to two detection cells, one of which was heated to 358 K to enable dissociation of $N_2O_5$ to $NO_3$.

However, a more recent, and time-resolved, study by Lewis *et al.*,[9] using flash photolysis coupled to UV-Vis absorption detection, reports that little $NO_3$ is generated from the formaldehyde oxide + $NO_2$ reaction and that the observed $NO_3$ can be rationalized by reaction of $INO_2$ with $IONO_2$, yielding $NO_3$ alongside $NO_2$ and $I_2$.

Inconsistencies within the literature regarding $NO_3$ as a major product of Criegee + $NO_2$ reactions must lead to consideration of other potential products. In the reaction of Criegee intermediates with carboxylic acids, Criegee-acid adducts were postulated as reaction products.[10] Earlier work performed in this laboratory on the acetaldehyde oxide + $NO_2$ system at 4 Torr lead to the observation of a weak, yet temporally-resolved, and $NO_2$-dependent signal at the mass of the Criegee-$NO_2$ adduct (106.01 amu).[3] The channel leading to this adduct formation (1b) is in direct competition with $NO_3$ production (1a), and so if present, would significantly affect the anticipated $NO_3$ yield, and hence the atmospheric impact of this reaction. In this work, we further interrogate the products and rate coefficients for $NO_2$ reactions with formaldehyde-oxide and acetaldehyde-oxide in the range 4-40 Torr using MPIMS and assess the potential atmospheric impact on $NO_x$/$NO_y$ chemistry through global modelling.

**Experimental details**

Experiments were performed using a Multiplexed Photoionization Mass Spectrometer (MPIMS) installed with one of two halocarbon-wax coated quartz reactor tubes to allow operating pressures of up to 10 Torr (650 μm pinhole) or up to 40 Torr (300 μm pinhole), both at room temperature.[11] He, $O_2$, $NO_2$ (1 % in He) and the Criegee precursor (diiodomethane or 1,1-diiodoethane, entrained in a flow of He via a pressure- and temperature-regulated bubbler), were delivered to the reactor via a set of calibrated mass-flow controllers. The reaction was initiated via photolysis at 248 nm, where the cross section of $NO_2$ is at a minimum,[12, 13] using an excimer laser aligned collinearly with the flow of gas through the reactor, the pressure of which was maintained via a feedback-controlled butterfly valve. Reaction products were sampled via the pinhole into a low pressure region, where quasi-continuous photoionization using the tunable synchrotron radiation output from the Chemical Dynamics Beamline of the Advanced Light Source at Lawrence Berkeley National Laboratory enabled detection via an orthogonal acceleration time-of-flight mass spectrometer.[14, 15]

Two types of measurements were made using this apparatus: single energy measurements at either 10.5 or 13.0 eV to obtain kinetic data, and measurements of time-resolved photoionization spectra. In the latter, the ionization photon energy was scanned in 25 meV steps to obtain 3-dimensional (photon energy, mass-to-charge ratio (m/z), and kinetic time) data sets. This allows for isomeric resolution using calculated or measured reference photoionization energy spectra, which are unique to each molecule.[11, 16] Some additional experiments to verify the source of the Criegee-$NO_2$ adduct were performed using the broadband ionizing radiation output of a $H_2$ discharge lamp fitted with a $MgF_2$ filter, which effectively limits the output energy range to ~8.5-10.3 eV.

Pseudo-first-order conditions were maintained so that $[NO_2]>>[Criegee]$. In order to minimize the contribution of RCR'I + $NO_2$ and favor RCR'I + $O_2$, $[O_2]$ was held in excess of $[NO_2]$.[4]

**Theoretical details**

Experimental measurements were complimented by *ab initio* calculations of minimum energy adduct structures and adiabatic ionization energies (AIE), which serve as estimates for the onset

of the experimental photoionization spectrum. Minimum energy structures of the previously proposed acetaldehyde oxide-$NO_2$ adduct (m/z = 106),[3] have been optimized at the ωB97XD/6-31+G(d) level of density functional theory.[17-22] To aid comparison with experiment, the adiabatic and vertical ionization energies (VIE) of each isomer were calculated as the zero-point energy-inclusive energy difference between the neutral radical and the cation form. The cation geometry used for AIE calculation was obtained by optimization started from the optimized neutral geometry, while that used for VIE was a single point cation calculation at the geometry of the neutral.

Further calculations have been performed on $CH_3CHIOONO_2$, and all structures relating to this species have been optimized using ωB97XD functional[17, 18] and the ADZP basis set.[23, 24]

**Model description**

The global chemistry transport model used in this study, STOCHEM, is a 3-dimensional Chemical Transport Model (CTM) in which 50,000 constant mass air parcels are advected every three hours by wind using a Lagrangian approach allowing the chemistry and transport processes to be uncoupled. STOCHEM is an 'offline' model with the transport and radiation codes driven by archived meteorological data, generated by the UK Meteorological Office Unified Model (UM) at a grid resolution of 1.25° longitude, 0.8333° latitude, and 12 unevenly spaced (with respect to altitude) vertical levels with an upper boundary of 100 hPa .[25] A detailed description of the vertical coordinate, advection scheme, and dispersion processes used in STOCHEM can be found in Collins *et al.*,[26] with updates described by Derwent *et al.*[27] The chemical mechanism used in STOCHEM is the common representative intermediates mechanism version 2 and reduction 5 (CRI v2-R5), referred to as 'STOCHEM-CRI'. The detail of the CRI v2-R5 mechanism is given by Jenkin *et al.*,[28] Watson *et al.*,[29] and Utembe *et al.*,[30] with updates highlighted in further publications by Utembe *et al.*[31, 32] The emissions data employed in the base case STOCHEM model were adapted from the Precursor of Ozone and their Effects in the Troposphere (POET) inventory for the year 1998.[33] More details about the emissions data can be found in Khan *et al.*[34] The concentration of stabilized Criegee intermediates are integrated with STOCHEM-CRI and was calculated using the steady state approximation method with the total production rate

equal to $k_x[\text{alkene}_x][O_3]\alpha$ (where $k_x$ is the rate coefficient for the reaction of $\text{alkene}_x$ with ozone and α is the fraction of stabilized Criegee intermediates formed) and the total loss rate equal to ($k_2 + k_3[H_2O]$) (where $k_2$ is the unimolecular loss rate for a stabilized Criegee intermediate, assigned a value of 100 $s^{-1}$ for all Criegee intermediates, and $k_3$, set to $1 \times 10^{-16}$ molecule$^{-1}$ cm$^3$ $s^{-1}$ for all Criegee intermediates, is the rate coefficient for the reaction of the CI with $H_2O$). The loss of Criegee intermediates due to reaction of $CH_2OO$ with water dimer is rapid,[9, 35] so we excluded the contribution of $CH_2OO$ in the calculation of the total concentration of stabilized Criegee intermediates. The formation of $NO_3$ from the reaction of stabilized Criegee intermediates with $NO_2$ ($k_1 \sim 2.0 \times 10^{-12}$ molecule$^{-1}$ cm$^3$ $s^{-1}$) is compared to the formation from the reaction of $O_3$ with $NO_2$.

**Results and discussion**

*Kinetics*

Pseudo-first-order rate coefficients (*k'*) for the reaction of acetaldehyde oxide with $NO_2$ were obtained by fitting the temporal profiles of acetaldehyde oxide with single exponential decays with a y-axis offset, convolved with an instrument response function.[7, 36, 37] Kinetic measurements were performed at a fixed photoionization energy of 10.5 eV, where the signal is thought to arise mainly from the *syn*-conformer of acetaldehyde oxide.[3] Temporal profiles of acetaldehyde oxide in the absence and presence of $NO_2$ are shown in Figure 1, demonstrating that the removal rate is enhanced with increasing $NO_2$ concentration. Weighted linear fits to plots of the pseudo-first-order rate coefficient for Criegee intermediate loss against $NO_2$ concentration yielded bimolecular rate coefficients for the reaction at 20 and 40 Torr (Figure 2).

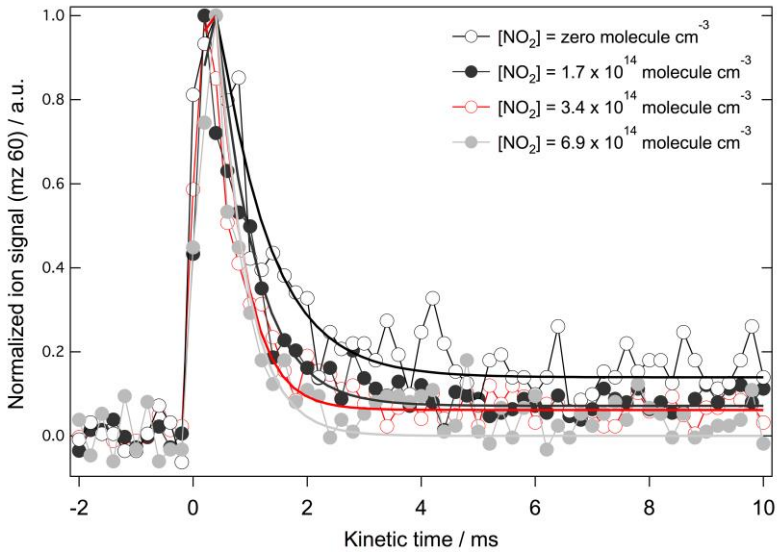


**Figure 1**: Temporal profiles of acetaldehyde oxide (m/z 60) in the presence of $NO_2$, measured at a total pressure of 40 Torr and 300 K and an ionization energy of 10.5 eV. Kinetic data fitted with single exponential decays with a y-axis offset, convoluted with the instrument response function.

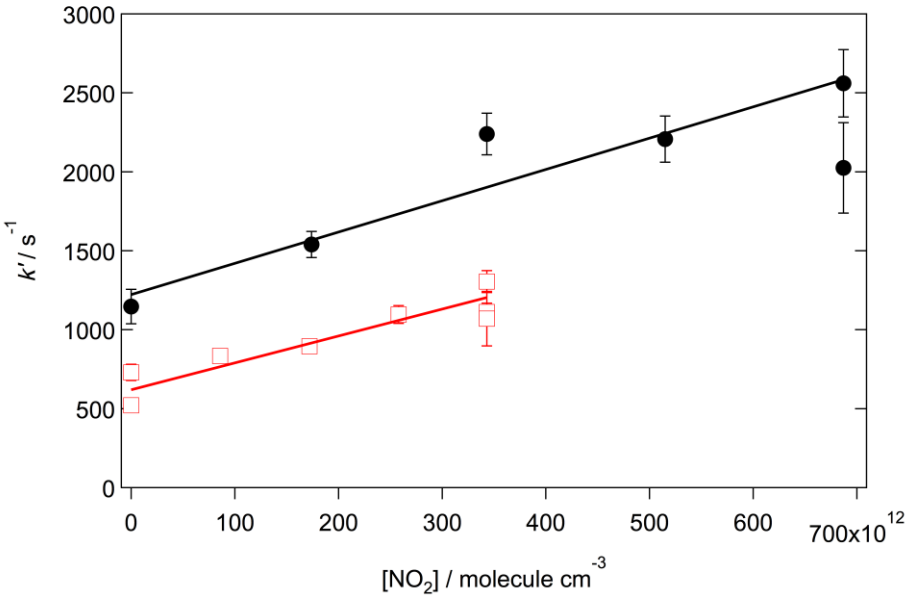


**Figure 2**: Pseudo-first-order rate coefficients obtained from single exponential decay fits to the acetaldehyde oxide signal as a function of $[NO_2]$. Bimolecular rate coefficients (see Table 1) are obtained by with linear fits to the data, weighted to the 1σ error bars. Red squares: 20 Torr. Black circles: 40 Torr.

The measured bimolecular rate coefficients (Table 1) are comparable to the rate coefficients reported by Stone *et al.* (formaldehyde oxide),[4] Taatjes *et al.* (acetaldehyde oxide),[3] and Chhantyal-Pun *et al.* (acetone oxide).[2]

**Table 1:** Measured rate coefficients for the reaction of acetaldehyde oxide with $NO_2$ alongside other Criegee + $NO_2$ rate coefficients reported in the literature. Values obtained from linear, weighted fits to the bimolecular plots, and reported errors are the 95 % confidence intervals of the fits.

| Criegee | | *P* /Torr | $k$ / $10^{-12}$ molecule$^{-1}$ cm$^3$ s$^{-1}$ |
|---|---|---|---|
| Formaldehyde oxide | Welz *et al.*[7] | 4 | 7 (+3, -2) |
| | Stone *et al.*[4] | 25-300 | 1.5 ± 0.5 |
| Acetaldehyde oxide | Taatjes *et al.*[3] | 4 | 2 ± 1 |
| | This work | 20 | 1.7 ± 0.3 |
| | | 40 | 2.0 ± 0.7 |
| Acetone oxide | Chhantyal-Pun *et al.*[2] | 4 | ≤ 5 |

The rate coefficient for formaldehyde oxide + $NO_2$ was not obtained because of the inability to differentiate between the two co-reactants due to insufficient mass resolution ($CH_2OO$ is 46.005 amu and $NO_2$ is 45.993 amu) and because the ionization onset energy for the excess reactant $NO_2$ (9.586 eV) is below that of formaldehyde oxide (~ 10 eV),[7, 38] preventing isolation of $CH_2OO$ based on ionization energy.

*Investigation of $NO_3$ formation*

The previously proposed products of the acetaldehyde oxide + $NO_2$ reaction are acetaldehyde and $NO_3$. The observed acetaldehyde signal, normalized for number of laser shots, was found to *decrease* as a function of increasing $NO_2$ concentration, which is consistent with the observations of Stone *et al.*[4] in the study of formaldehyde oxide + $NO_2$ reaction and of Chhantyal-Pun *et al.*[2] in the acetone oxide + $NO_2$ reaction (Figure 3).

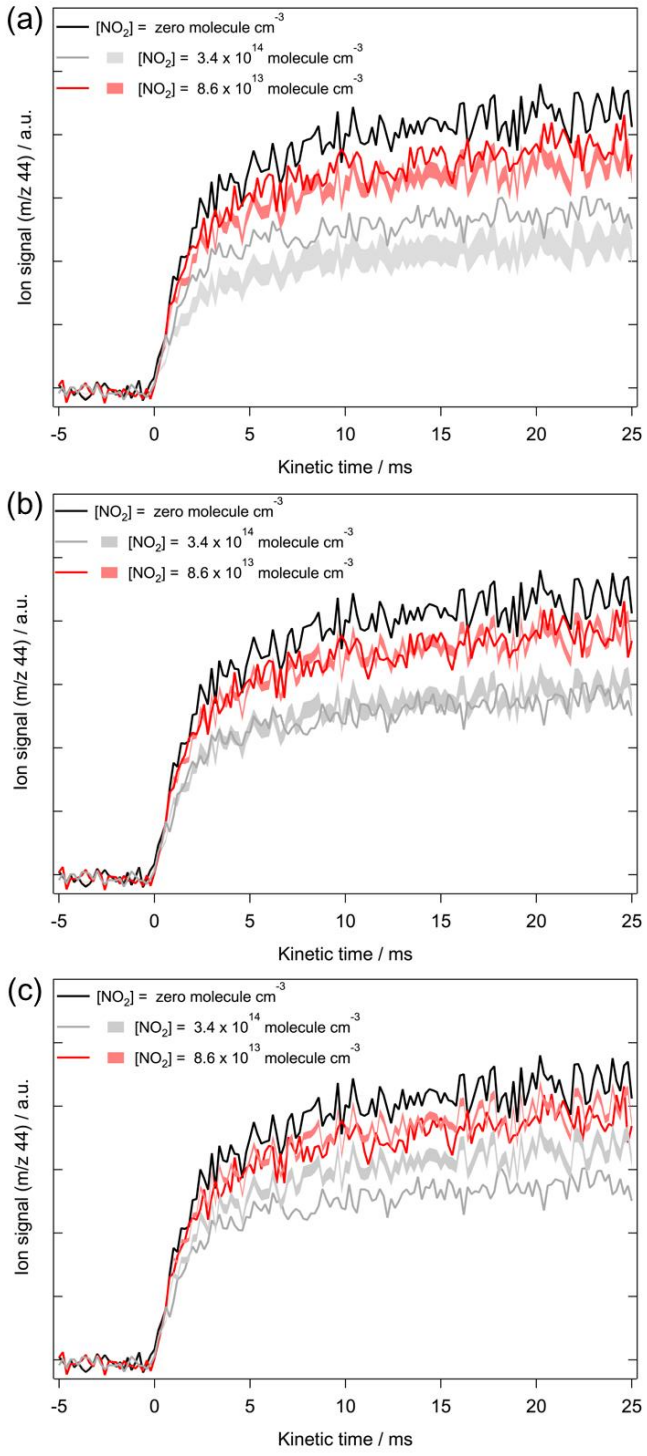


**Figure 3**: Temporal profiles of acetaldehyde (m/z 44) in the presence of $NO_2$, measured at a total pressure of 20 Torr and 300 K and an ionization energy of 10.5 eV. The experimental data are shown alongside modelled acetaldehyde signal assuming (a) 0% yield of (R1a) (b) 30 % of (R1a) and (c) 50 % of (R1a). Other potential contributions to the acetaldehyde signal, such as the reaction of $CH_3CHIO_2$ + I, are not accounted for in this qualitative analysis.

Based on the rate coefficient for acetaldehyde oxide + $NO_2$ at 20 Torr, reported in this work (Table 1) and the acetaldehyde signal observed in the absence of $NO_2$, the anticipated signal at a given $NO_2$ concentration can be estimated, where the upper and lower limits are defined by the 95 % confidence intervals of the rate coefficient. Assuming a 0 % yield of (R1a), the modelled acetaldehyde signal is below that of the observed experimental signal in the presence of $NO_2$ (Figure 8a). When a 30 % yield of (R1a) is accounted for (Figure 8b), the observed and modelled signals are within the bounds of one another, and so an upper limit of 30 % of (R1a) is feasible. If a 50 % yield of (R1a) is adopted (Figure 8c), the amplitudes of modelled signals are substantially above those of the measured signals, suggesting that the yield of acetaldehyde from (R1) is significantly below 50 %.

However, other pathways to formation of acetaldehyde are possible, for example the reaction of $CH_3CHIOO$ + I, yielding I + IO + acetaldehyde (which is rapid in the equivalent formaldehyde oxide system, according to Gravestock *et al.*[39]). At 20 Torr, the yield of $CH_3CHIOO$ from the reaction of $CH_3CHI$ + $O_2$ is estimated to be in the range 7-34 % based on experiments for the equivalent formaldehyde oxide system by Stone *et al*.[40] Therefore, the acetaldehyde signals will likely include a contribution from the $CH_3CHIOO$ + I reaction. As all products of this reaction can be obtained through multiple chemical pathways following photolysis of diiodoalkanes, we cannot quantitatively assess the effect of the reaction. Any acetaldehyde production method that is not effectively quenched by $NO_2$ would increase the apparent yield.

Detection of $NO_3$, the assumed co-product of the corresponding aldehyde from aldehyde-oxide + $NO_2$ reaction, would be a key observation; but $NO_3$ has eluded detection in time-resolved experiments on the elementary kinetics of such systems. To our best knowledge, no absolute photoionization cross-section measurements for $NO_3$ exist in the literature. However, Monks *et al.* [41] report an unscaled photoionization spectrum, which demonstrated a photoionization onset energy of 12.57 eV, with a maximum in the cross section obtained at ~12.7-12.8 eV. Single energy measurements were performed in this work at 13.0 eV of $NO_2$ in the presence of formaldehyde oxide ($3.9 \times 10^{14}$ molecule $cm^{-3}$ $NO_2$ at 30 Torr) and acetaldehyde oxide (1.5-6.9 ×

$10^{14}$ molecule $cm^{-3}$ $NO_2$ at 4-40 Torr), respectively. However, no time-resolved signal at the parent mass of $NO_3$ (m/z 62) could be observed.

Although the $NO_3$ photoionization cross-section remains unknown, estimates based on NO (1.7 Mb at 10.5 eV) and $NO_2$ (0.2 Mb at 10.5 eV) suggest that the cross-section could be small. Assuming that the cross-section of $NO_3$ is as small as that of $NO_2$, we estimate that we could readily detect ~ $3 \times 10^{11}$ molecule $cm^{-3}$ of $NO_3$. This would correspond to ~ 10-15 % of our estimated initial acetaldehyde oxide concentration, which is lower than, but consistent with the upper limit we derive based on the acetaldehyde depletion at 20 Torr (Figure 8). However, $NO_3$ loss through secondary chemistry would reduce its peak concentration, and possibly hinder its direct detection.

We have attempted to measure secondary products of $NO_3$ but have found no unambiguous evidence. In the study of Ouyang *et al.*[8] it was thought that $NO_3$ was largely titrated to $N_2O_5$. Although in the present study the reactor residence times are much shorter (~40-140 ms, cf. ~3.2 s), some reaction with $NO_2$ is still possible. The potential presence of $N_2O_5$ was investigated at 13.0 eV (photoionization onset energy reported at ~11.4-12.3 eV),[42, 43] but no time-resolved signal was observed at the parent mass of $N_2O_5$ (107.98 amu). Kinetic studies of the reactions of $NO_3$ with I and $I_2$ by Chambers *et al.*[44] has shown these reactions to be fast ($4.5 \times 10^{-10}$ and $1.5 \times 10^{-12}$ $molecule^{-1}$ $cm^3$ $s^{-1}$) and lead to the formation of IO + $NO_2$, and I + $IONO_2$ respectively. Under the present experimental conditions, it is estimated that ~ 16 % of $NO_3$ would be lost via reaction with $NO_2$, and the remainder mainly via reaction with I.[44, 45] The signal of IO (Figure 4), which is also produced from the reactions of Criegee with I, and RCR'IOO with I, is found to decrease as $NO_2$ concentration is increased, and is removed more rapidly at higher $NO_2$ concentrations. An increase in IO with increasing $NO_2$ could be an indication of $NO_3$ formation, but without quantification of the other sources of IO, the observed decrease is ambiguous.

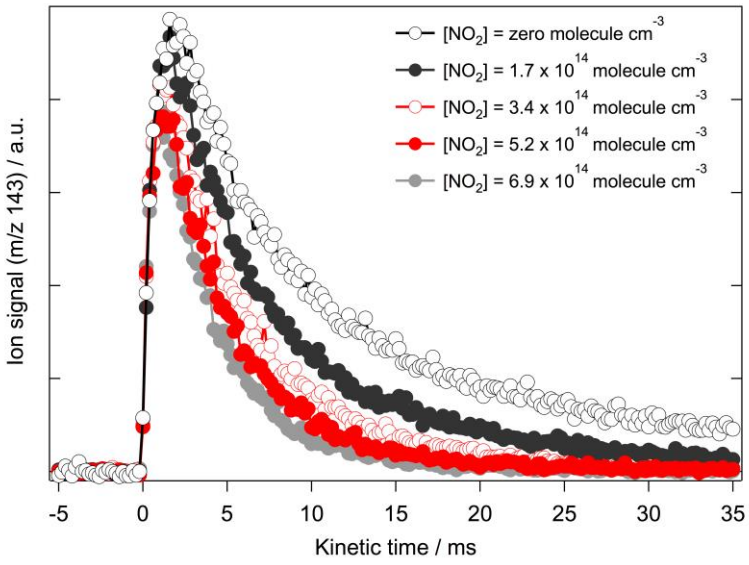


**Figure 4**: Temporal profiles of IO (m/z 143) in the presence of $NO_2$, measured at a total pressure of 40 Torr and 300 K, and an ionization energy of 10.5 eV.

The reaction of $I_2$ with $NO_3$ leads to the formation of $IONO_2$, but the recombination of I atoms to produce $I_2$ is slow enough in the present system that this reaction would not be competitive with the reaction of I with $NO_3$ under our experimental conditions.[44, 46] Nevertheless a weak, time-resolved signal at the $IONO_2$ parent mass is indeed observed under our experimental conditions (formaldehyde oxide + $NO_2$, 30 Torr, $[NO_2] = 3.9 \times 10^{14}$ molecule $cm^{-3}$). However, the reaction of IO + $NO_2$ (~ $3.2 \times 10^{-13}$ molecule$^{-1}$ $cm^3$ $s^{-1}$ at 30 Torr of He[47-49]) is a more likely source of the $IONO_2$ signal due to $NO_2$ being an excess reagent in our system. A reference photoionization spectrum of $INO_3$ is unavailable, and so the observed signal cannot be quantified, nor verified as a parent mass signal as opposed to a daughter ion of a larger species. The $INO_3$ signal is therefore also not a reliable reporter for $NO_3$ formation.

*$NO_2$-facilitated isomerization*

Following investigations into acetone oxide reactions, Chhantyal-Pun *et al.*[2] reported evidence for $SO_2$- or $NO_2$-assisted isomerization of acetone-oxide to 2-hydroxypropene and methyldioxirane. This was manifested in the long-time signal (foot) of the m/z 74 ion signal

increasing relative to the peak maximum as a function of increasing co-reactant. In the present work, single energy measurements recorded at 10.5 eV, where acetaldehyde oxide and vinylhydroperoxide are both ionized,[3, 50] demonstrate that over the entire pressure range studied (4-40 Torr), the relative height of the foot decreases as a function of increasing $NO_2$. Therefore, there is no evidence in the present study for substantial $NO_2$-facilitated isomerization of acetaldehyde oxide.

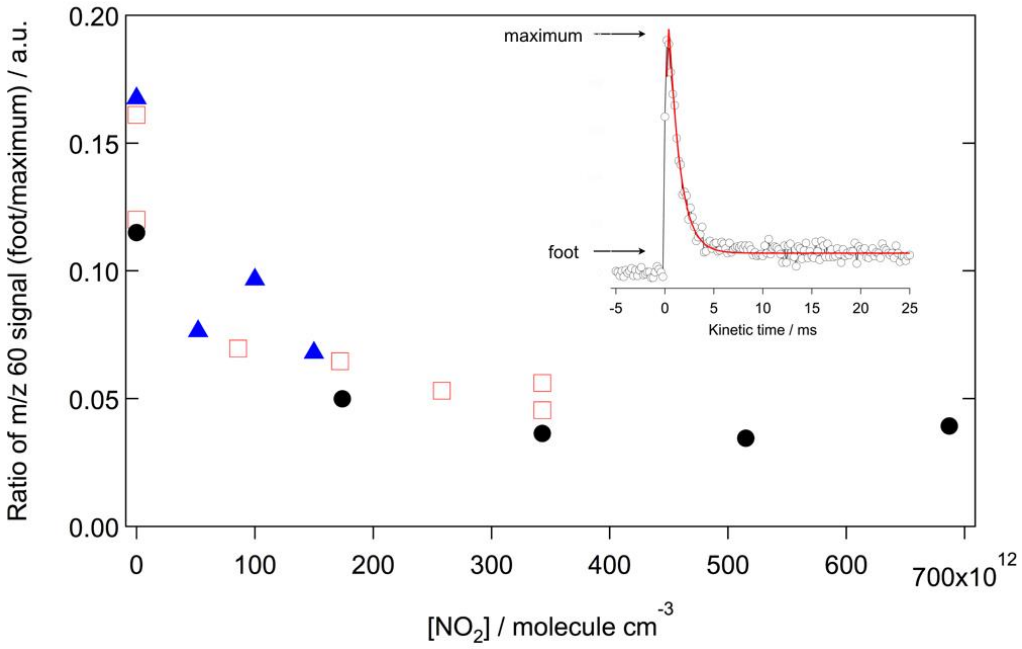


**Figure 5**: Ratio of signal heights of the long-time y-axis offset (foot) to the maximum signal height for m/z 60 (see inset), as a function of [$NO_2$]. Blue triangles: 4 Torr. Red open squares: 20 Torr. Black circles: 40 Torr.

*Investigation of Crigee-$NO_2$ adduct formation*

Previous studies have yielded evidence for the formation of an adduct between Criegee intermediates and $NO_2$.[3] In the present work, the formation of this association product was investigated for the reactions of $NO_2$ with both formaldehyde oxide and acetaldehyde oxide in the 4-40 Torr pressure range. Clear time-resolved and [$NO_2$]-dependent signals were observed at the parent masses of both adducts, $CH_2OONO_2$ (91.998 amu) and $CH_3CHOONO_2$ (106.014 amu), respectively, across the investigated pressure range (Figures 6 and 7) and were found to

monotonically increase with $[NO_2]$. The m/z axis was calibrated using a mixture of ethane, propene, 1-butene and xenon.

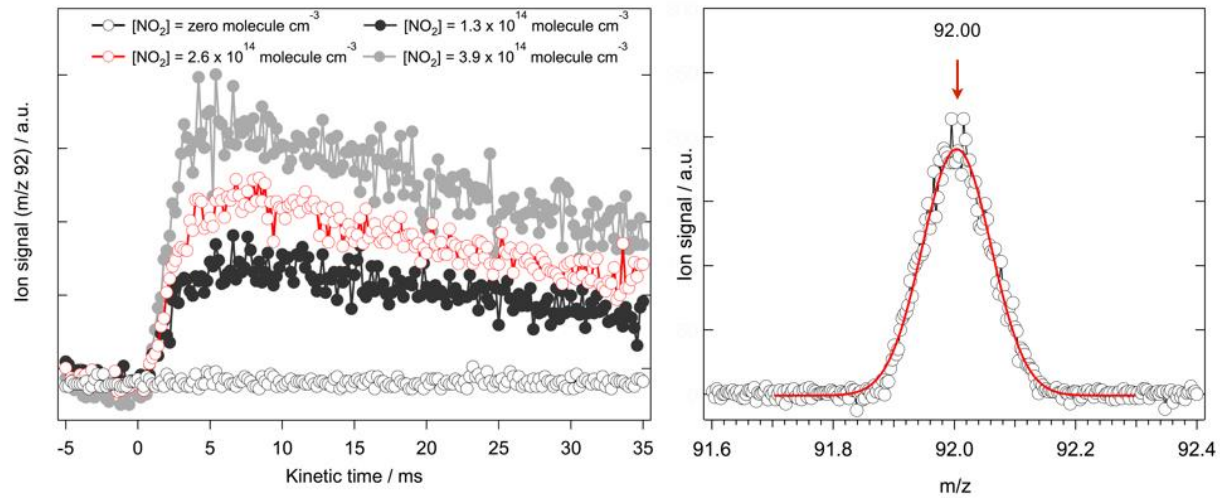


**Figure 6**: Left - Temporal profiles of $CH_2OONO_2$ (m/z 92) from the reaction of formaldehyde oxide + $NO_2$, measured at a total pressure of 30 Torr and 300 K, and an ionization energy of 10.5 eV. Right – Integrated ion signal of m/z 92, fitted with a Gaussian function (red line) to yield the exact mass of 92.00 amu.

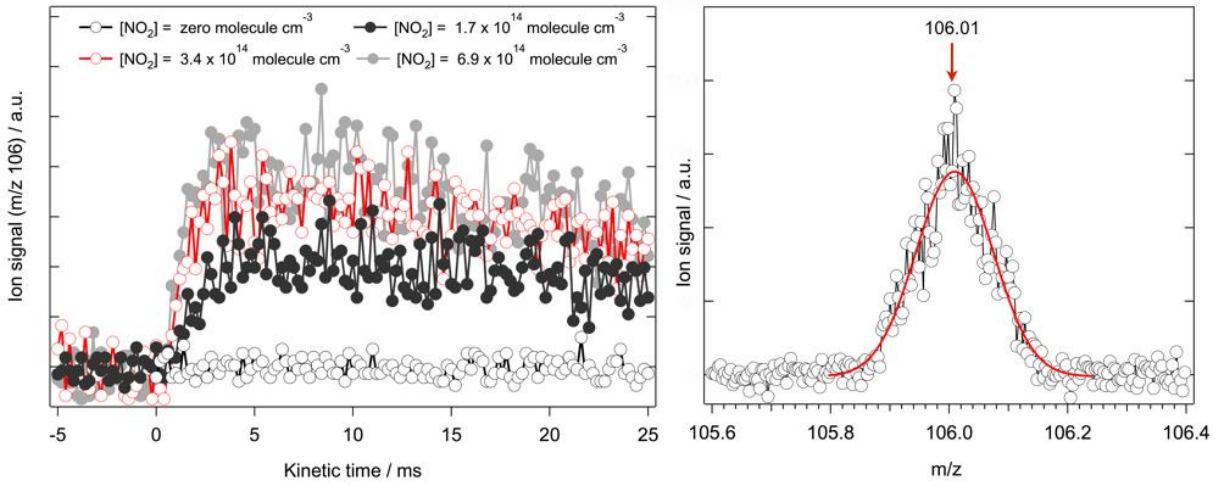


**Figure 7**: Left - Temporal profiles of $CH_3CHOONO_2$ (m/z 106) from the reaction of acetaldehyde oxide + $NO_2$, measured at a total pressure of 40 Torr and 300 K, and an ionization energy of 10.5 eV. Right – Integrated ion signal of m/z 106, fitted with a Gaussian function (red line) to yield the exact mass of 106.01 amu.

Photoionization energy spectra were obtained for signals at the mass of the $CH_2OONO_2$ (92 amu) and $CH_3CHOONO_2$ (106 amu) adducts, from the reactions of $NO_2$ with formaldehyde oxide and acetaldehyde oxide both at 40 Torr, respectively, and are shown in Figure 8.

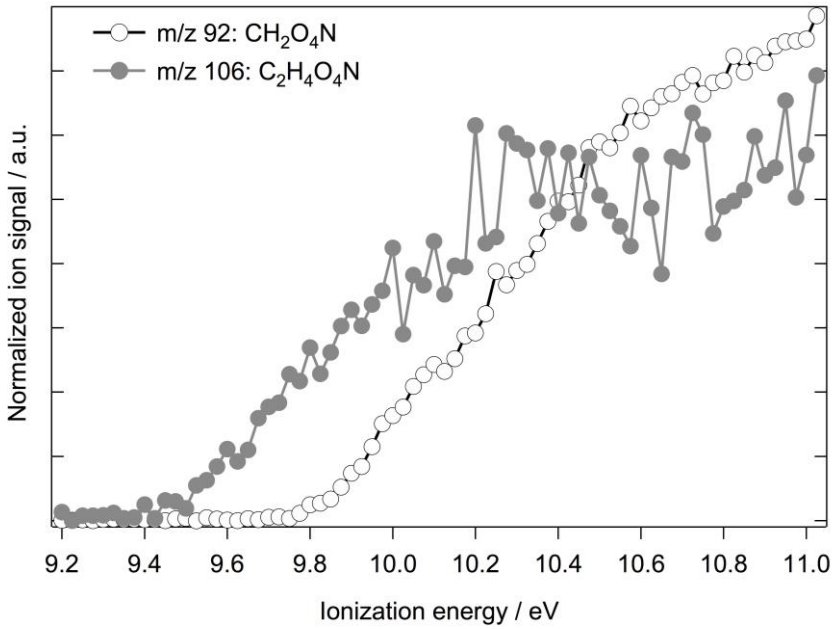


**Figure 8**: Measured photoionization energy curves for the adduct species m/z 92 from the formaldehyde oxide + $NO_2$ reaction (black) and m/z 106 from the acetaldehyde oxide + $NO_2$ reaction (gray, scaled for ease of comparison), both measured at 40 Torr, 300 K with 25 meV resolution. The data are normalized for the number of laser shots, and the photon flux of the synchrotron radiation at each energy.

*Ab initio* calculations were performed (as described in the Theoretical details section) to obtain possible structures which potentially lead to the m/z 106 signal from the acetaldehyde oxide + $NO_2$ reaction, and four structures were identified. These structures, their zero-point vibrational energy inclusive energy, and adiabatic ionization energy values are listed in Figure 9.

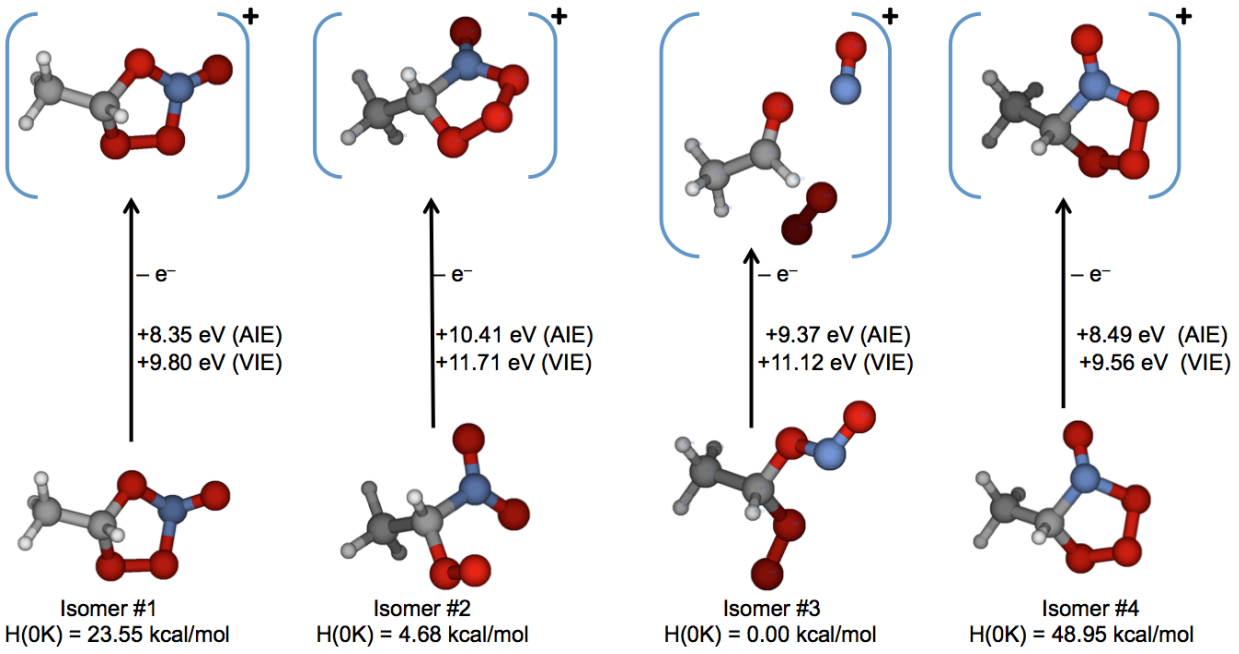


**Figure 9**: Possible isomers of $CH_3CHOONO_2$ adduct optimized at the ωB97XD/6-31+G(d) level along with the zero-point-inclusive energy [kcal/mol], and their adiabatic ionization energy [eV]. It is notable that the onset of the m/z 106 signal corresponds roughly to the AIE value calculated for the isomer #3, however this is predicted to lead to an unbound cation, in conflict with the present observation at the parent mass.

The failure to detect $NO_3$ and the observed decrease in aldehyde signal with increasing [$NO_2$] suggests that the association adduct is the major product of Criegee + $NO_2$ reactions. From the exact mass of the adduct signal (Figures 6 and 7), it is clear that the temporally-resolved and $NO_2$ -dependent signals comprise the chemical formulae consistent with $CH_2OONO_2$ and $CH_3CHOONO_2$ from the formaldehyde oxide and acetaldehyde oxide systems. However, we carried out further verification of the origin of these chemical species. Besides the reaction of Criegee with $NO_2$, there are again other potential sources that require consideration, for example, reactions of iodoalkyl peroxy radicals:

$$RCR'IOO + NO_2 \longrightarrow RCR'IOONO_2 \xrightarrow{D.I.} [RCR'OONO_2]^+ + I \qquad \text{(R2a)}$$

$$RCR'IOO + NO_2 \longrightarrow RCR'OONO_2 + I \qquad \text{(R2b)}$$

The formation of iodoalkylperoxy radicals (RCR'IOO) occurs from the reaction of iodoalkyl (RCR'I) with $O_2$, and is in direct competition with Criegee intermediate formation.

$$RCR'I + O_2 \longrightarrow RCR'OO + I \quad \text{(R3a)}$$

$$RCR'I + O_2 \longrightarrow RCR'IOO \quad \text{(R3b)}$$

The yield of formaldehyde oxide from iodoalkyl + $O_2$ reaction as a function of pressure was investigated by Stone *et al.*,[40] who obtained yields in the range of 68-99 % at 4 Torr, decreasing to 64-86 % at 40 Torr. Therefore, the reactions of iodoalkylperoxy radicals will be increasingly prominent at higher pressures where their yield from R3 is enhanced. The estimated rate coefficient for iodoalkylperoxy radicals with $NO_2$ is on the order of the rate coefficient for Criegee intermediate + $NO_2$ reactions, measured in this and previous work.[4] Therefore, the potential role of R2 cannot be excluded based only on kinetics.

The first product channel (R2a), whereby $RCR'OONO_2^+$ is formed as a daughter ion of $RCR'IO_2NO_2$ via dissociative ionization (D.I.), can be differentiated theoretically from the second, direct ionization product of $RCR'OONO_2$ parent, by comparison of calculated photoionization onset energies with measured photoionization spectra. Optimization of the cation form of $CH_3CHIO_2NO_2$, the acetaldehyde oxide analogue of $RCR'IO_2NO_2$, from the optimized neutral structure leads to a bound cation with an adiabatic ionization energy of 9.61 eV (Figure 10). The ionization energy at which this neutral structure yields $CH_3CHO_2NO_2^+$ via R2a was calculated to be 10.51 eV – far above the measured onset of m/z 106 (~ 9.4 eV). Therefore, it is unlikely that dissociative ionization of $RCR'IO_2NO_2$ leads to the observed signal at the Criegee-$NO_2$ adduct mass.

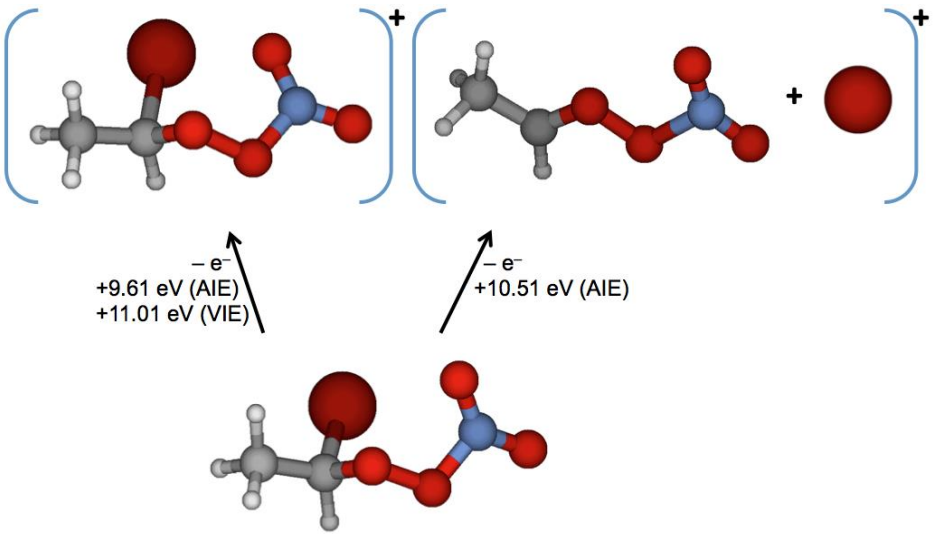


**Figure 10**: Calculated ionization energies of the $CH_3CHIO_2NO_2$ structure, optimized at the ωB97XD/ADZP level, leading to a bound cation, and to $CH_3CHO_2NO_2^+$ + I.

To investigate the potential contribution of the second channel R2b to RCR'OONO$_2$ formation, acetaldehyde oxide + $NO_2$ experiments were performed in the presence of $SO_2$. Kinetic measurements of acetaldehyde oxide with $SO_2$ have shown a nearly gas-kinetic rate coefficient, and so $SO_2$ would act as a scrubber for Criegee intermediates, removing them before they can react with $NO_2$.[3, 4, 7, 10] If the adduct signal were to persist in the presence of $NO_2$ and the scrubber, this would demonstrate that the adduct formation is due to side chemistry, such as R2, and not the reaction of interest. Recent work by Huang *et al.*[51] demonstrated that the reaction of $CH_2IOO$ with $SO_2$ is rapid, but a factor of 10 slower than $CH_2OO$ + $SO_2$. Addition of $SO_2$ therefore will remove both Criegee intermediates and RCR'IOO, but at sufficiently different rates so that the source of the adduct signals can be determined. Therefore, the specific amount of depletion of the adduct by a given $SO_2$ concentration acts as a test – the removal rates of $CH_3CHIOO$ by $NO_2$ and by $SO_2$ are expected to be roughly equal, whereas for the Criegee intermediate $SO_2$ should be a factor of 10 (for *syn*-$CH_3CHOO$) or 100 (for *anti*-$CH_3CHOO$) more effective than $NO_2$. Figure 11 compares the signal at the adduct mass (normalized for the total number of laser shots) without $SO_2$ and with addition of $SO_2$ at 0.07 of the $NO_2$ concentration. If the signal were the product of a reaction of $CH_3CHIOO$, one would expect this small concentration of $SO_2$ to have a negligible effect. However, the signal at the adduct mass is

in fact reduced by ~30%, slightly less but similar to the ~50% reduction predicted by the ratio of rate coefficients for reaction of the Criegee intermediate with $SO_2$ and $NO_2$. This reduction suggests that the product probed at m/z 106 is substantially, if not entirely, due to reaction of the Criegee intermediate.

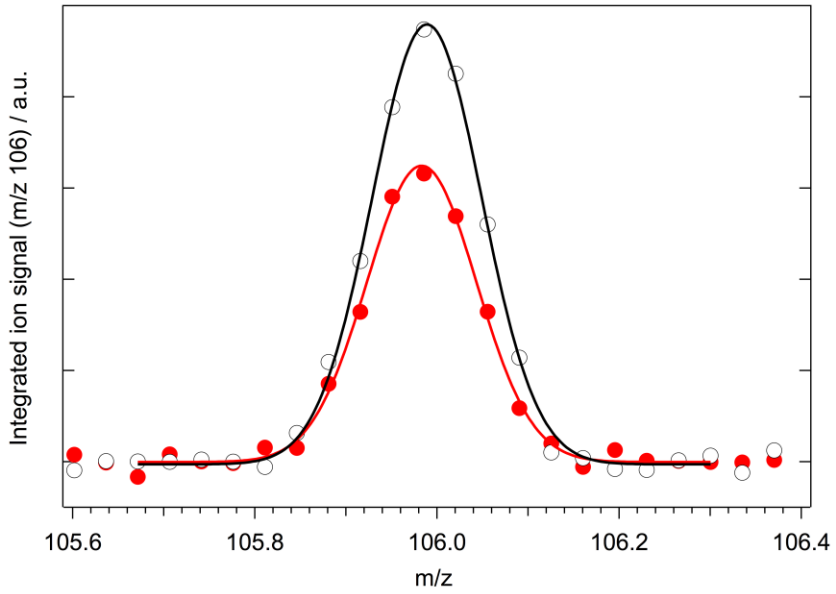


**Figure 11**: Integrated ion signal of m/z 106 (open circles) normalized for the number of laser shots, fitted with a Gaussian function (black and red lines) for the reaction of acetaldehyde oxide + $NO_2$ performed in the absence of (black open circles) and presence of (red open circles) $SO_2$.

**Atmospheric implications**

The integration of the global model (STOCHEM-CRI) after including the reaction (R1a) provides a small additional source of $NO_3$ in the troposphere (Figure 12a), which can alter the oxidizing capacity of the troposphere especially during night-time. The reaction channel (R1) acts as a sink for Criegee intermediates (Figure 12b), which would reduce their abundance mostly in North America, Central Europe, and South East Asia. Thus regardless of the product, this reaction channel is important to evaluate Criegee intermediate oxidative effects in the atmosphere. Compared with the production of $NO_3$ from the reaction of $NO_2$ and $O_3$ (the major production route for $NO_3$), if the reaction channel (R1a) were 100% of the yield, this reaction increases the surface $NO_3$ levels by a few percent globally and up to 5% in equatorial regions

particularly in South America due to larger abundances of Criegee intermediates derived from isoprene and monoterpenes (see Figure 12a). The increment of $NO_3$ shown in Figure 9a is found to be much lower than the estimation made in the earlier study by Taatjes *et al.*[3] study, but this small amount could still be significant for reassessing the global $NO_3$ budget and also be able to improve the ubiquitous under-predictions of $NO_3$ in high-alkene areas. However, the present results show no evidence for $NO_3$ formation, indicating rather that adduct formation is likely the dominant product channel. If we consider adduct formation (R1b) from Criegee intermediate + $NO_2$ as a competitor of $NO_3$ production (R1a) in the model, the anticipated $NO_3$ yield will be even lower than shown in Figure 12a, making the reaction of Criegee intermediates a smaller perturbation on nitrate concentration, unless the adduct in turn generates $NO_3$.

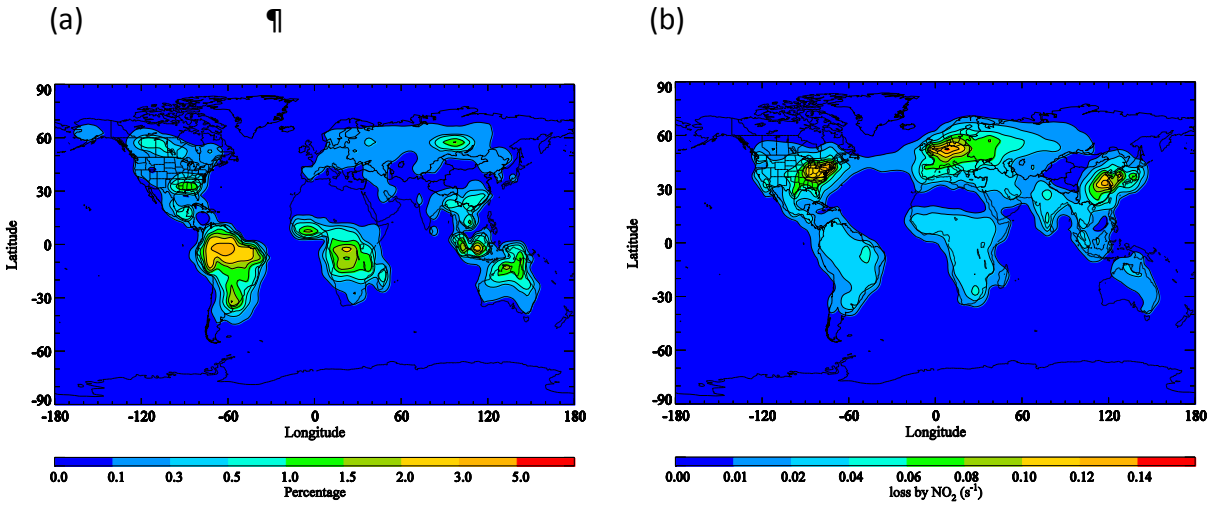


**Figure 12:** (a) Annual surface distribution of increased $NO_3$ (in percent form) for the addition of production route of $NO_3$ through Criegee intermediates. (b) Fraction of Criegee intermediate loss that is attributable to reaction with $NO_2$ based on the present and literature rate coefficients.

## Conclusions

The reactions of formaldehyde- and acetaldehyde-oxide Criegee intermediates with $NO_2$ have been examined between 4 and 40 Torr using a Multiplexed Photoionization Mass Spectrometer (MPIMS) coupled to tunable synchrotron radiation. The postulated reaction product, $NO_3$, could not be detected, however a species consistent with the exact Criegee-$NO_2$ mass was observed

in both systems, with increasing signal as a function of $NO_2$ concentration. It is postulated that this adduct is the major reaction product, and based on the acetaldehyde signal an upper limit of ~ 30 % is placed on the $NO_3$ + acetaldehyde yield. The fate of these Criegee-$NO_2$ adducts requires further investigation to fully understand the impact of this reaction on tropospheric $NO_x$.

**Acknowledgements**

This material is based upon work supported by the Division of Chemical Sciences, Geosciences and Biosciences, Office of Basic Energy Sciences (BES), U.S. Department of Energy (USDOE). Sandia National Laboratories is a multiprogram laboratory operated by Sandia Corporation, a Lockheed Martin Company, for the USDOE's National Nuclear Security Administration under contract DEAC04-94AL85000. We thank Raybel Almeida for his technical assistance with the MPIMS experiments. This research used resources of the Advanced Light Source of Lawrence Berkeley National Laboratory, which is a USDOE Office of Science User Facility. The Advanced Light Source is supported by the Director, Office of Science, BES/USDOE, under contract DE-AC02- 05CH11231 between Lawrence Berkeley National Laboratory and the USDOE.

**References**


1. R. G. Prinn, *Annual Review of Environment and Resources*, 2003, 28, 29-57.
2. R. Chhantyal-Pun, O. Welz, J. D. Savee, A. J. Eskola, E. P. Lee, L. Blacker, H. R. Hill, M. Ashcroft, M. A. H. Khan, G. C. Lloyd-Jones, L. Evans, B. Rotavera, H. Huang, D. L. Osborn, D. K. W. Mok, J. M. Dyke, D. E. Shallcross, C. J. Percival, A. J. Orr-Ewing and C. A. Taatjes, *The Journal of Physical Chemistry A*, 2016.
3. C. A. Taatjes, O. Welz, A. J. Eskola, J. D. Savee, A. M. Scheer, D. E. Shallcross, B. Rotavera, E. P. F. Lee, J. M. Dyke and D. K. W. Mok, *Science*, 2013, 340, 177-180.
4. D. Stone, M. Blitz, L. Daubney, N. U. Howes and P. Seakins, *Physical Chemistry Chemical Physics*, 2014, 16, 1139-1149.
5. L. Vereecken, H. Harder and A. Novelli, *Physical Chemistry Chemical Physics*, 2012, 14, 14682-14695.
6. A. A. Presto and N. M. Donahue, *The Journal of Physical Chemistry A*, 2004, 108, 9096-9104.
7. O. Welz, J. D. Savee, D. L. Osborn, S. S. Vasu, C. J. Percival, D. E. Shallcross and C. A. Taatjes, *Science*, 2012, 335, 204-207.
8. B. Ouyang, M. W. McLeod, R. L. Jones and W. J. Bloss, *Physical Chemistry Chemical Physics*, 2013, 15, 17070-17075.
9. T. R. Lewis, M. A. Blitz, D. E. Heard and P. W. Seakins, *Physical Chemistry Chemical Physics*, 2015, 17, 4859-4863.
10. O. Welz, A. J. Eskola, L. Sheps, B. Rotavera, J. D. Savee, A. M. Scheer, D. L. Osborn, D. Lowe, A. Murray Booth, P. Xiao, M. A. H. Khan, C. J. Percival, D. E. Shallcross and C. A. Taatjes, *Angewandte Chemie International Edition*, 2014, 53, 4547-4550.
11. D. L. Osborn, P. Zou, H. Johnsen, C. C. Hayden, C. A. Taatjes, V. D. Knyazev, S. W. North, D. S. Peterka, M. Ahmed and S. R. Leone, *Review of Scientific Instruments*, 2008, 79, 104103.
12. S. P. Sander, R. Friedl, D. Golden, M. Kurylo, G. Moortgat, P. Wine, A. Ravishankara, C. Kolb, M. Molina and B. Finlayson-Pitts, Jet Propulsion Laboratory, California Institute of Technology Pasadena, California, Chemical kinetics and photochemical data for use in atmospheric studies evaluation number 15, 2006.
13. A. C. Vandaele, C. Hermans, P. C. Simon, M. Carleer, R. Colin, S. Fally, M.-F. Merienne, A. Jenouvrier and B. Coquart, *Journal of Quantitative Spectroscopy and Radiative Transfer*, 1998, 59, 171-184.
14. D. L. Osborn and C. A. Taatjes, *International Reviews in Physical Chemistry*, 2015, 34, 309-360.
15. J. D. Savee, S. Soorkia, O. Welz, T. M. Selby, C. A. Taatjes and D. L. Osborn, *The Journal of Chemical Physics*, 2012, 136, 134307.
16. C. A. Taatjes, N. Hansen, D. L. Osborn, K. Kohse-Höinghaus, T. A. Cool and P. R. Westmoreland, *Physical Chemistry Chemical Physics*, 2008, 10, 20-34.
17. J.-D. Chai and M. Head-Gordon, *The Journal of Chemical Physics*, 2008, 128, 084106.
18. J.-D. Chai and M. Head-Gordon, *Physical Chemistry Chemical Physics*, 2008, 10, 6615-6620.
19. P. C. Hariharan and J. A. Pople, *Theoretica chimica acta*, 1973, 28, 213-222.

20. T. Clark, J. Chandrasekhar, G. W. Spitznagel and P. V. R. Schleyer, *Journal of Computational Chemistry*, 1983, 4, 294-301.
21. R. Krishnan, J. S. Binkley, R. Seeger and J. A. Pople, *The Journal of Chemical Physics*, 1980, 72, 650-654.
22. P. M. Gill, B. G. Johnson, J. A. Pople and M. J. Frisch, *Chemical Physics Letters*, 1992, 197, 499-505.
23. P. De Oliveira, C. Barros, F. Jorge, A. C. Neto and M. Campos, *Journal of Molecular Structure: THEOCHEM*, 2010, 948, 43-46.
24. A. C. Neto, E. P. Muniz, R. Centoducatte and F. E. Jorge, *Journal of Molecular Structure: THEOCHEM*, 2005, 718, 219-224.
25. T. C. Johns, R. E. Carnell, J. F. Crossley, J. M. Gregory, J. F. Mitchell, C. A. Senior, S. F. Tett and R. A. Wood, *Climate dynamics*, 1997, 13, 103-134.
26. W. Collins, D. S. Stevenson, C. Johnson and R. Derwent, *Journal of Atmospheric Chemistry*, 1997, 26, 223-274.
27. R. Derwent, D. Stevenson, R. Doherty, W. Collins and M. Sanderson, *Atmospheric Environment*, 2008, 42, 7412-7422.
28. M. E. Jenkin, L. A. Watson, S. R. Utembe and D. E. Shallcross, *Atmospheric Environment*, 2008, 42, 7185-7195.
29. L. A. Watson, D. E. Shallcross, S. R. Utembe and M. E. Jenkin, *Atmospheric Environment*, 2008, 42, 7196-7204.
30. S. R. Utembe, L. A. Watson, D. E. Shallcross and M. E. Jenkin, *Atmospheric Environment*, 2009, 43, 1982-1990.
31. S. R. Utembe, M. C. Cooke, A. T. Archibald, M. E. Jenkin, R. G. Derwent and D. E. Shallcross, *Atmospheric Environment*, 2010, 44, 1609-1622.
32. S. R. Utembe, M. C. Cooke, A. T. Archibald, D. E. Shallcross, R. G. Derwent and M. E. Jenkin, *Atmospheric environment*, 2011, 45, 1604-1614.
33. C. Granier, J. Lamarque, A. Mieville, J. Muller, J. Olivier, J. Orlando, J. Peters, G. Petron, G. Tyndall and S. Wallens, POET, a database of surface emissions of ozone precursors, 2005.
34. M. A. H. Khan, M. C. Cooke, S. R. Utembe, P. Xiao, R. G. Derwent, M. E. Jenkin, A. T. Archibald, P. Maxwell, W. C. Morris and N. South, *Atmospheric Environment*, 2014, 99, 77-84.
35. W. Chao, J.-T. Hsieh, C.-H. Chang and J.-J. M. Lin, *Science*, 2015, 347, 751-754.
36. C. A. Taatjes, *International Journal of Chemical Kinetics*, 2007, 39, 565-570.
37. S. B. Moore and R. W. Carr, *International Journal of Mass Spectrometry and Ion Physics*, 1977, 24, 161-171.
38. S. Lias, in *Ionization Energy Evaluation in NIST Chemistry WebBook, NIST Standard Reference Database Number 69* eds. P. Linstrom and W. Mallard, National Institute of Standards and Technology, Gaithersburg MD.
39. T. J. Gravestock, M. A. Blitz, W. J. Bloss and D. E. Heard, *ChemPhysChem*, 2010, 11, 3928-3941.
40. D. Stone, M. Blitz, L. Daubney, T. Ingham and P. Seakins, *Physical Chemistry Chemical Physics*, 2013, 15, 19119-19124.

41. P. Monks, L. Stief, M. Krauss, S. Kuo, Z. Zhang and R. Klemm, *The Journal of Physical Chemistry*, 1994, 98, 10017-10022.
42. D. Ames and D. Turner, *Proceedings of the Royal Society of London A: Mathematical, Physical and Engineering Sciences*, 1976, 348, 175-186.
43. S. G. Lias, J. E. Bartmess, J. F. Liebman and J. L. Holmes, in *NIST Chemistry WebBook, NIST Standard Reference Database Number 69*, eds. R. Levin and W. Mallard, National Institute of Standards and Technology,, Gaithersburg MD, 2003, vol. 20899.
44. R. Chambers, A. Heard and R. Wayne, *The Journal of Physical Chemistry*, 1992, 96, 3321-3331.
45. R. Atkinson, D. L. Baulch, R. A. Cox, J. N. Crowley, R. F. Hampson, R. G. Hynes, M. E. Jenkin, M. J. Rossi and J. Troe, *Atmos. Chem. Phys.*, 2004, 4, 1461-1738.
46. D. Baulch, J. Duxbury, S. Grant and D. Montague, *J. Phys. Chem. Ref. Data*, 1981, 10.
47. E. Daykin and P. Wine, *Journal of Physical Chemistry*, 1990, 94, 4528-4535.
48. F. Maguin, G. Laverdet, G. Le Bras and G. Poulet, *The Journal of Physical Chemistry*, 1992, 96, 1775-1780.
49. S. P. Sander, G. W. Ray and R. T. Watson, *The Journal of Physical Chemistry*, 1981, 85, 199-210.
50. F. Liu, Y. Fang, M. Kumar, W. H. Thompson and M. I. Lester, *Physical Chemistry Chemical Physics*, 2015, 17, 20490-20494.
51. M. Huang, T. A. Miller, N. D. Kline and R. Dawes, *The Journal of Physical Chemistry A*, 2016, DOI: 10.1021/acs.jpca.6b10632.